ORIGINAL PAPER

Assessment of Radial Basis Function Network Method for Fractal-Like Agglomerate Dynamics

Chang Ma[1] · Mingzhou Yu[1] ©

Abstract

During physical and chemical processes, aerosol particles often undergo coagulation to form Agglomerates. Agglomerates are fractal-like in a statistical sense, whose dynamical evolution of particle size distribution is governed by the population balance equation (PBE). In this study, the Radial Basis Function (RBF) method RBF is firstly extended to the solution of fractal-like agglomerate dynamics problems. The applicable conditions, and advantages and disadvantages of this method are studied. Two dynamic processes of fractal-like agglomerates, namely Brownian coagulation in the continuum regime and Brownian coagulation in the free molecular regime, are investigated. As a comparison, the sectional method (SM) is utilized as the referenced method. The initial geometric standard deviation (GSD) and the fractal dimension (D_f) of agglomerates are found to be the two main key factors affecting the accuracy and efficiency of the RBF. The RBF method is more suitable for calculating cases with larger GSD. As the GSD increases (i.e., GSD > 1.2), the computational efficiency and accuracy of the RBF increase accordingly. The RBF method is more suitable for calculating cases with larger D_f. As the D_f decreases, the calculation error of RBF method becomes further larger, which is more obvious in the free molecular regime. Compared with the SM method, the calculation efficiency of RBF method increases by 3–4 orders of magnitude. This study provides excellent application of RBF method to the solution of the PBE.

List of symbols

D_f	Fractal dimension
M_k	Kth moment of agglomerate size distribution
N_0	Initial agglomerate number concentration
r	The number of Gauss–Laguerre points
s	The number of Gauss–Legendre points
v_{g0}	The initial mean volume
t	Time
u_k	kth Gauss–Laguerre point position
$u_k\prime$	kth Gauss–Legendre point position
$\tilde{v}, v$	Agglomerate volume
w_k	kth Gauss-Laguerre point weight
$w_k\prime$	kth Gauss–Legendre point weight

Greek letters

σ_0	Initial geometric standard deviation
β	Collision kernel

✉ Mingzhou Yu
  mzyu@cjlu.edu.cn

1   Laboratory of Aerosol Science and Technology, China
    Jiliang University, Xueyuan Street 258, Hangzhou 310018,
    Zhejiang, China

1 Introduction

Aerosol particles tend to aggregate into agglomerates of varying sizes through physical and chemical processes, with diameters typically ranging from several nanometers to 0.1 μm (Hinds and Zhu 2022). Under this condition, agglomerates are fractal-like in a statistical sense. The evolution of agglomerate size distribution is a very sensitive function of agglomerate structure, volume loading and process conditions. Due to its fractal property, the dynamics of agglomerate has absolutely different characteristics relative to the coagulation process of coalescing particles, which can be calculated by solving the classical Smoluchowski equation using an appropriate expression for the collision kernel (Yu and Lin 2009b). It is found as the idea of fractal theory is introduced into the power law relationship between agglomerate and primary particles, the classical Smoluschowski

equation, shown in Eq. (2), can be also applied to study the dynamics of agglomerates (Yu and Lin 2009b). Here, the power law relation is,

$$N_{\mathrm{p}} = \left(\frac{v_c}{v_{\mathrm{p}0}} \right)^{\mathrm{D}_f} \tag{1}$$

where N_{p} is the number of primary particles in an agglomerate, v_c is the particle collision volume and $v_{\mathrm{p}0}$ the radius of primary particle and D_f the mass fractal dimension (or Hausdorff dimension). For compact spherical agglomerates, the Hausdorff dimension is 3, while for chain-like structure the Hausdorff dimension is 1.

The classical Smoluschowski equation, only involving coagulation process, can be seen as a simplified form of the well-known population balance equation (PBE) (Jeldres et al. 2018). The PBE can describe particle evolution under all kinds of processes (i.e., advection, diffusion, coagulation, nucleation, surface growth, and other physical or chemical phenomena, etc.). In a statistical sense, the evolution of nanoparticles, whether is spherical or fractal, in air or solution is controlled by PBE, which is a highly nonlinear partial differential equation (Friedlander 2000). However, it is computationally demanding to directly solve the PBE mainly because of its dependence on the particle volume (Xie et al. 2012). Since the PBE is a complex integral differential equation, obtaining its analytical solution is challenging. Nevertheless, various numerical solution methods have been developed and used (Yu et al. 2016), such as the sectional method (SM) (Rodrigues et al. 2018; Yu et al. 2017), the moment method (MOM) (Fox et al. 2022; Yu et al. 2008), the Monte Carlo method (Apelgren et al. 2019), and so on. Each of the commonly used PBE numerical methods has its advantages and limitations. SM has the highest precision and the highest time cost. The moment method can maintain high accuracy and speed, but the result obtained by the moment method is only the statistics of the particles, and there are errors in the variation law of particle size distribution (PSD) obtained by using statistical information.

The idea of combining radial basis functions with collocation methods to solve numerical solutions of partial differential equations has been successfully applied in many fields (Mirzaei 2020; Motaman et al. 2018). In Wang's study (Wang et al. 2020), the RBF theory was first applied to solve the PBE, and it achieved favorable results. Later, Alzyod et al. (2020) used the multiple quadratic basis function to convert PBE into the form of ordinary differential equations. They used the Runge–Kutta method to solve the particle growth, nucleation, coagulation and breakage problems. In another of their studies (Alzyod 2021), they proposed that the adaptive radial basis function is used to the hydrodynamics of liquid–liquid dispersions. Adaptive radial

basis functions alleviate the problems of steep gradients and wide ranges during particle coagulation and breakage. Later, Wang used the log-Gaussian function as the basis function to calculate problems such as Brownian coagulation and self-preserving distribution (Wang et al. 2022). The advantage of the RBF method is that the evolution of the PSD over time can be obtained directly, and this method is a mesh-free method. As far as we know, there is no report on the application of RBF in agglomerate dynamics problems. Especially, as the fractal theory is introduced to the PBE, whether RBF is suitable for solving problems such as PBE equations is still unknown.

In this article, the RBF method is extended to the Brownian coagulation equation for fractal-like agglomerates. The coagulation kernel in agglomerate systems is different from spherical particle systems in mathematical structure. Whether the RBF is applicable to the study of this type of collision kernel needs to be further clarified. More importantly, as a new powerful method for solving the PBE, there is still a lot of specific work, including the applicability conditions of this method, the advantages and disadvantages compared with other methods, etc., still need further confirmation.

The purpose of this article is to further investigate the RBF method. The range of parameters suitable for the calculation of the RBF method was studied, including initial GSD and fractal dimension, D_f. The reason for the influence of these parameters on the RBF method are analyzed. The remainder of this article is organized as follows. In Sect. 2, the theory about the RBF is presented. In this section, how to use the RBF to solve the PBE is described in detail. In Sect. 3, the computational condition and parameters are presented. In Sect. 4, the accuracy of the RBF method and its suitable computational range were investigated. And a brief comparison of computational speeds was conducted. This is followed by some concluding remarks in Sect. 5.

2 Theory

Smoluchowski gave the calculation equation of particle number concentration in a multiphase flow system in 1917 (Smoluchowski 1918). This equation was further improved by Müller later (Müller 1928), and the continuous form of the equation was given. Its continuous form is as follows:

$$\frac{\partial n(v,t)}{\partial t} = \frac{1}{2} \int_0^v \beta(\tilde{v}, v - \tilde{v}) n(\tilde{v}, t) n(v - \tilde{v}, t) \mathrm{d}\tilde{v} - n(v, t) \int_0^\infty \beta(\tilde{v}, v) n(\tilde{v}, t) d\tilde{v} \tag{2}$$

the above equation is known as the Smoluchowski coagulation equation or the population balance equation (PBE). $n(v, t)\mathrm{d}v$ is the number of particles whose volume is

between v and $v + dv$ at time t, $\beta(\tilde{v}, v)$ is the collision kernel function between the volumes v and $\tilde{v}$.

In Mountain's research (Mountain et al. 1986), the fractal dimension parameter was successfully applied to the particle collision equation. The form of collision kernel in the free molecular regime is as follows:

$$\beta(v, \tilde{v}) = K \left(v^{\frac{1}{D_f}} + \tilde{v}^{\frac{1}{D_f}} \right)^2 \left(\frac{1}{v} + \frac{1}{\tilde{v}} \right)^{\frac{1}{2}} \tag{3}$$

The form of collision kernel in the continuum regime is as follows:

$$\beta(v, \tilde{v}) = K \left(v^{\frac{1}{D_f}} + \tilde{v}^{\frac{1}{D_f}} \right) \left(v^{-\frac{1}{D_f}} + \tilde{v}^{-\frac{1}{D_f}} \right) \tag{4}$$

where K is the collision kernel coefficient, v and $\tilde{v}$ are the particle volume. D_f is the fractal dimension. By adjusting the parameter D_f, the PSD of agglomerates with various fractal structures can be calculated.

Using the RBF method to approximate the PBE, $n(v, t)$ should be constructed as follows:

$$n(v, t) = n_{\text{init}}(v) + t n^*(v, t) \tag{5}$$

where $n_{\text{init}}(v)$ is the initial distribution of the equation, t is the time, and $n^*(v, t)$ is the objective function to be approximated using the RBF method. The meaning of Eq. (5) is to make the approximate result satisfy the initial distribution.

To solve PBE by using RBF method, it is necessary to choose appropriate basis functions. Three parameters need to be determined, namely the center position of the basis function, the standard deviation (width), and the weight.

For the choice of the basis function, the Gaussian function is chosen here. As $n^*(v, t)$ to be approximated depends on both variables v and t, the RBF method uses a two-dimensional Gaussian distribution as the basis function. Since the variables v and t are independent of each other, $n^*(v, t)$ can be expressed as follows:

$$n^*(v, t) = \frac{1}{v} \sum_{i=1}^{p} \sum_{j=1}^{q} w_{ij} \varphi_i(v) \psi_j(t) \tag{6}$$

where $\frac{1}{v}$ is a coefficient produced by the log transformation, p is the number of basis functions in the volume dimension. q is the number of basis functions in the time dimension. There are total $p \times q$ basis functions. w_{ij} is the weight corresponding to the (i, j) th basis function, φ_i is the i th basis function corresponding to the volume dimension, and ψ_j is the j th basis function corresponding to the time dimension. The forms of φ_i and ψ_j are as follows:

$$\varphi_i(\ln v) = \exp \left[-\frac{\ln^2 (v/v_i)}{2\sigma_v^2} \right] \tag{7}$$

$$\psi_j(t) = \exp \left[-\frac{(t-t_j)^2}{2\sigma_t^2} \right] \tag{8}$$

The center location of the basis function is selected using the uniform distribution. In Eq. (7), σ_v, and in Eq. (8), σ_t, denote the standard deviation of the Gaussian distribution. The standard deviation defines the shape of the basis function and is formulated as follows:

$$\sigma_v = \frac{2(\ln V_{\max} - \ln V_{\min})}{p-1} \tag{9}$$

$$\sigma_t = \frac{2T}{q-1} \tag{10}$$

Figure 1 shows the image of the two-dimensional Gaussian distribution as the basis function.

With the transformations described above, Eq. (5) can be approximated as a weighted sum of basis functions, represented as follows:

$$n(v, t) \approx \tilde{n}(v, t) = n_{\text{init}}(v) + \frac{t}{v} \sum_{i=1}^{p} \sum_{j=1}^{q} \lambda_{ij} \varphi_i(v) \psi_j(t) \tag{11}$$

The PBE contains the partial derivative term and the integral term. For the partial derivative term on the left side of Eq. (2), the form after derivation is as follows:

$$\frac{\partial \tilde{n}(v,t)}{\partial t} = \frac{1}{v} \sum_{i=1}^{p} \sum_{j=1}^{q} \lambda_{ij} \varphi_i(v) \psi_j(t) + \frac{t}{v} \sum_{i=1}^{p} \sum_{j=1}^{q} \lambda_{ij} \varphi_i(v) \psi_j'(t) \tag{12}$$

the form of $\psi_j'(t)$ is as follows:

$$\psi_j'(t) = \frac{t_j - t}{\sigma_t^2} \exp \left[-\frac{(t-t_j)^2}{2\sigma_t^2} \right] \tag{13}$$

The algorithm needs to discretize the two integral terms on the right side of the Eq. (2). The first integral term after the
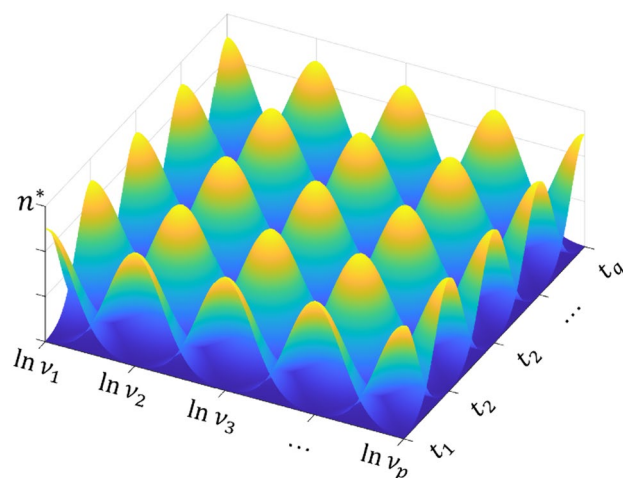

Fig. 1 Basis function distribution

equal sign is discretized using the Gauss-Laguerre quadrature method. The discrete result using the Gauss-Laguerre integral method is as follows:

$$\frac{1}{2} \int_0^v \beta(\tilde{v}, v - \tilde{v}) n(\tilde{v}, t) n(v - \tilde{v}, t) d\tilde{v}$$

$$\approx \underbrace{\frac{v}{4} \sum_{k=1}^s \beta\left(\frac{v}{2} - \frac{v}{2}u_k, \frac{v}{2} + \frac{v}{2}u_k\right) \tilde{n}\left(\frac{v}{2} - \frac{v}{2}u_k, t\right) \tilde{n}\left(\frac{v}{2} + \frac{v}{2}u_k, t\right) w_k}_{S_1(v,t)}$$

(14)

where s is the number of Gauss-Laguerre points, u_k is the position of the kth integral point, and w_k is the weight of the kth integral point.

The second integral term after the equal sign is discretized using the Gaussian-Legendre quadrature method. The discrete result using the Gauss–Legendre integral method is as follows:

$$n(v, t) \int_0^\infty \beta(\tilde{v}, v) n(\tilde{v}, t) d\tilde{v} \approx \tilde{n}(v, t) \underbrace{\sum_{k=1}^r e^{u'_k} \beta\left(v, u'_k\right) \tilde{n}\left(u'_k, t\right) w'_k}_{S_2(v,t)}$$

(15)

where r is the number of Gauss–Legendre points, u'_k is the position of the kth integral point, and w'_k is the weight of the kth integral point.

This method updates w_{ij} using the Levenberg–Marquardt optimization algorithm. The mean square error (MSE) is used as the evaluation standard to measure the accuracy of the model in the iterative process and its form is as follows:

$$Loss = \frac{1}{pq} \sum_{i=1}^p \sum_{j=1}^q \left(\frac{\partial \tilde{n}(v_i, t_j)}{\partial t} - S_1\left(v_i, t_j\right) + S_2\left(v_i, t_j\right)\right)^2 \quad (16)$$

Throughout the RBF method's training, the training data coincides in both position and quantity with the centers of the basis functions. With each iteration of the LM algorithm, the loss decreases, allowing the model to progressively conform to PBE constraints.

3 Computations

The numerical computations are all performed on an Intel i7-8700 CPU 3.2 GHz computer with memory 16 GB and all numerical computation schemes of RBF method are run in MATLAB 2018. For the referenced SM, the section number is 500 and the time step is 0.001.

4 Result

4.1 Agglomerates Coagulation in the Continuum Regime

Given that agglomerates size distributions often exhibit a log-normal distribution, the initial conditions used for this calculation are as follows:

$$n(v, t) = \frac{N_0}{3\sqrt{2\pi}v \ln \sigma_0} \exp\left[-\frac{\ln^2\left(\frac{v}{v_{g0}}\right)}{18 \ln^2 \sigma_0}\right] \quad (17)$$

where σ_0 is the initial geometric standard deviation, N_0 is the initial particle number concentration, and v_{g0} is the initial geometric mean volume. Here the parameters are chosen to be $N_0 = 1$, $\sigma_0 = 1.5$, $v_{g0} = 1$, and $K = 1$. The number of center points for v and t, i.e., p and q, are 30 and 10, respectively. The calculation ranges are $v \in \left[10^{-3}, 10^2\right]$ and $t \in [0, 1]$. The number of integration points for s and r are both 30. This parameter value does not represent the optimal choice. Within a certain range, the more the number of center points, the higher the calculation accuracy, but the corresponding calculation cost will also increase. To verify the accuracy of the calculation results, this method uses the SM (Vemury and Pratsinis 1995) as a contrast instead of the moment method.

Figure 2 displays the evolution of agglomerate size under various D_f values calculated using both the RBF method and SM method in the continuum regime.

The computational results from the two methods in Fig. 2 are highly consistent. To evaluate the accuracy of the RBF method, the root mean square error (RMSE) is
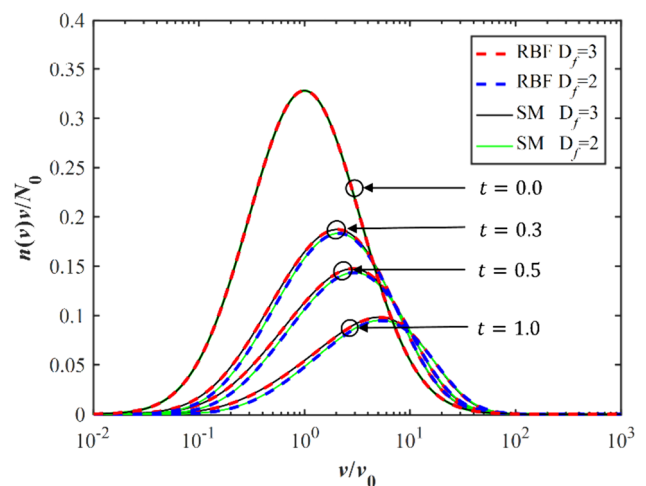
Fig. 2 In the continuum regime, the evolution of PSD over time for various D_f is predicted using both the RBF method and the sectional method

being used as a measure of error. The form of RMSE is as follows:

$$RMSE = \sqrt{\left(Y_{SM} - Y_{RBF}\right)^2} \tag{18}$$

where Y_{SM} is the PSD calculated by the SM method, and Y_{RBF} is the PSD calculated by the RBF method.

The RMSE for $D_f = 3$ and $D_f = 2$ are 1.1033e−4 and 1.4727e−04, respectively. These results suggest that the RBF method can still maintain accuracy when calculating the D_f from 2 to 3 in a limited region of the continuum regime.

In addition to directly calculating the evolution process of agglomerate size, the RBF method can also obtain moments of each order to analyze the evolution process of agglomerates. The k-order moment of agglomerate size distribution is as follows:

$$M_k = \int_0^\infty v^k n(v, t) dv \tag{19}$$

Figure 3 shows the calculated number concentration M_0 by the RBF method and the SM.

From Fig. 3, it can be observed that there is no significant disparity between the outcomes produced by the two methods. The moment computed through the RBF method can still maintain a high level of precision. The number concentration decreases over time. This is because Brownian coagulation constantly occurs between agglomerates, and smaller agglomerates form larger agglomerates through coagulation. The number of particles keeps decreasing, thus leading to a continuous decrease in particle number concentration. The decrease of D_f will lead to a faster
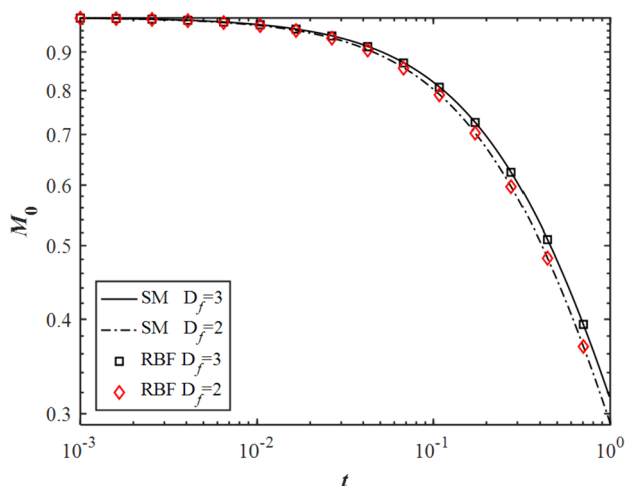
decline of number concentration. From the computational results, it can be observed that the influence of D_f on the particle number density function in the continuum regime is relatively small. This is consistent with the results of Yu (2009a).

4.2 Agglomerates Coagulation in the Free Molecular Regime

The initial distribution and parameters are consistent with those in Sect. 4.1. p and q are 30 and 10, and r and s are both 30. The calculated range is $v \in \left[10^{-3}, 10^2\right]$ and $t \in [0, 1]$.

Figure 4 shows the evolution of agglomerate size obtained by both the RBF and SM methods in the free molecular regime, with D_f ranging from 2 to 3. Since the SM method is difficult to calculate when init GSD = 1.5, $t = 1$, $D_f = 2$, this curve is not listed here.

Figure 4 displays the scale spectrum corresponding to D_f values of 3, 2.5, and 2. Their corresponding RMSE are 2.558e−04, 3.083e−04 and 5.079e−04, respectively. This indicates a high level of consistency in the computational results between the RBF and SM method in the free molecular regime. It suggests that employing the RBF method to compute finite regions with D_f ranging from 2 to 3 maintains high accuracy. The Fig. 4 shows that in the free molecular regime, the lower the value of D_f, the lower the corresponding density function at the same time. It also shows that the influence of D_f on the size evolution of agglomerates in the free molecular regime is greater than that in the continuum regime.

Figure 5 shows the calculated number concentration M_0 by the RBF method and the SM in the free molecular regime.
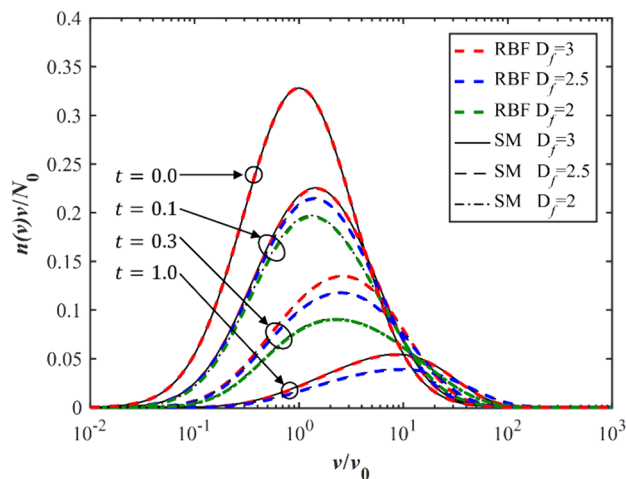

Fig. 3 In the continuum regime, the evolution of number concentration over time is predicted using the RBF method and the sectional method

Fig. 4 In the free molecular regime, the evolution of PSD over time for various D_f is predicted using both the RBF method and the sectional method
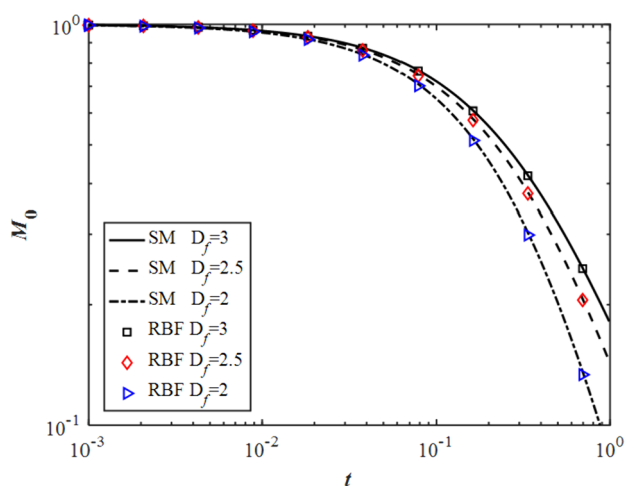
Fig. 5 In the free molecular regime, the evolution of number concentration over time is predicted using the RBF method and the sectional method

The comparison shows that the calculation results of this method are not significantly different from the SM. According to the Fig. 5, the number concentration in the free molecular regime keeps getting smaller with time. The smaller the D_f is, the faster the decay of particle number is. A decrease in the D_f value signifies a transformation of the agglomerate shape from spherical to platy and filamentous, indicating a more open structure of the agglomerates. This makes coagulation more likely to occur between the agglomerates. This result is consistent with the results of Yu (2009a).

4.3 Effect of Initial Geometric Standard Deviation Error Generation

Although the RBF method is capable of solving the particle number density function at lower computational costs, its efficiency is compromised when computing different initial GSD. In order to investigate the impact of the initial GSD on the calculations using this method, we computed cases with different GSD values. Other parameters remained consistent with those in Sect. 4.1. To measure the accuracy of the RBF method, the SM is used for comparison, and the RMSE after 100 iterations of the LM algorithm is used as the criterion for comparison.

The fundamental concept of the RBF method is to approximate the target function through a weighted sum of radial basis functions. Therefore, the study of the influence of different initial GSD values on the model should be conducted with a focus on the part related to the sum of weighted basis functions. $h(v, t)$ is defined as the weighted sum function of radial basis functions. Its form is as follows:

$$h(v,t) = \sum_{i=1}^{p} \sum_{j=1}^{q} \lambda_{ij} \varphi_i(\ln v) \psi_j(t) \tag{20}$$

Figure 6 shows the image of $h(v, t)$ with different initial GSD fitted by the RBF method.

According to the assumed normal distribution in Eq. (17), as σ_0 decreases, it implies a narrowing of the shape of the normal distribution. However, if we only consider the shape of the basis function weighted sum $h(v, t)$, the variation in the shape of $h(v, t)$ as σ_0 decreases is illustrated in Fig. 6. As the value of σ_0 decreases, the local gradients of the calculation results of $h(v, t)$ become larger. The variation in $h(v, t)$ leads to a mismatch in the shape of the basis functions, consequently impacting the accuracy of the model.

Figure 7 illustrates the RMSE curves obtained using the RBF method across various initial GSD within the continuum regime.

It can be seen from Fig. 7 that under the same initial conditions, RMSE gradually becomes larger with the decrease of σ_0. As the initial GSD decreases, the computational efficiency of RBF on PBE also decreases. This is caused by increasing gradient of the functions being fitted. Prior research has shown that approximating steep functions using RBF method is more challenging than approximating flat functions (Harris et al. 2017; Sarra and Bai 2018), the reason is that the radial basis function is essentially a local response function, each basis function has a strong response in its corresponding center and a certain range, and the response is very weak in other regions. When the local gradient of the objective function is large, the radial basis function of other regions responds weakly to this locality. This leads to an insufficient number of local basis functions. This will make it difficult for the RBF network to capture changes in these gradients. When the gradient of the function continues to rise, it may be necessary to increase the number of center points or adjust the shape of the basis function to ensure the speed and accuracy of the calculation (Kuo 2015). Therefore, the RBF method is more suitable for the case of large initial GSD.

To study the influence of the number of basis functions on the accuracy of the RBF method, the conditions outlined in Sect. 4.1 were chosen as a representative case for investigation. The calculated RMSE is as follows:

Figure 8 shows that as the number of basis functions increases, the calculation error continues to become smaller, and the error does not change significantly after the number of basis functions exceeds a certain value. These results indicate that for cases with a small initial GSD, increasing the number of basis functions by a certain amount can enhance the accuracy of the RBF method (Uddin 2014).

Previous studies have revealed that the shape of basis functions significantly influences the computational outcome (Bayona et al. 2011; Sarra and Sturgill 2009). In the process
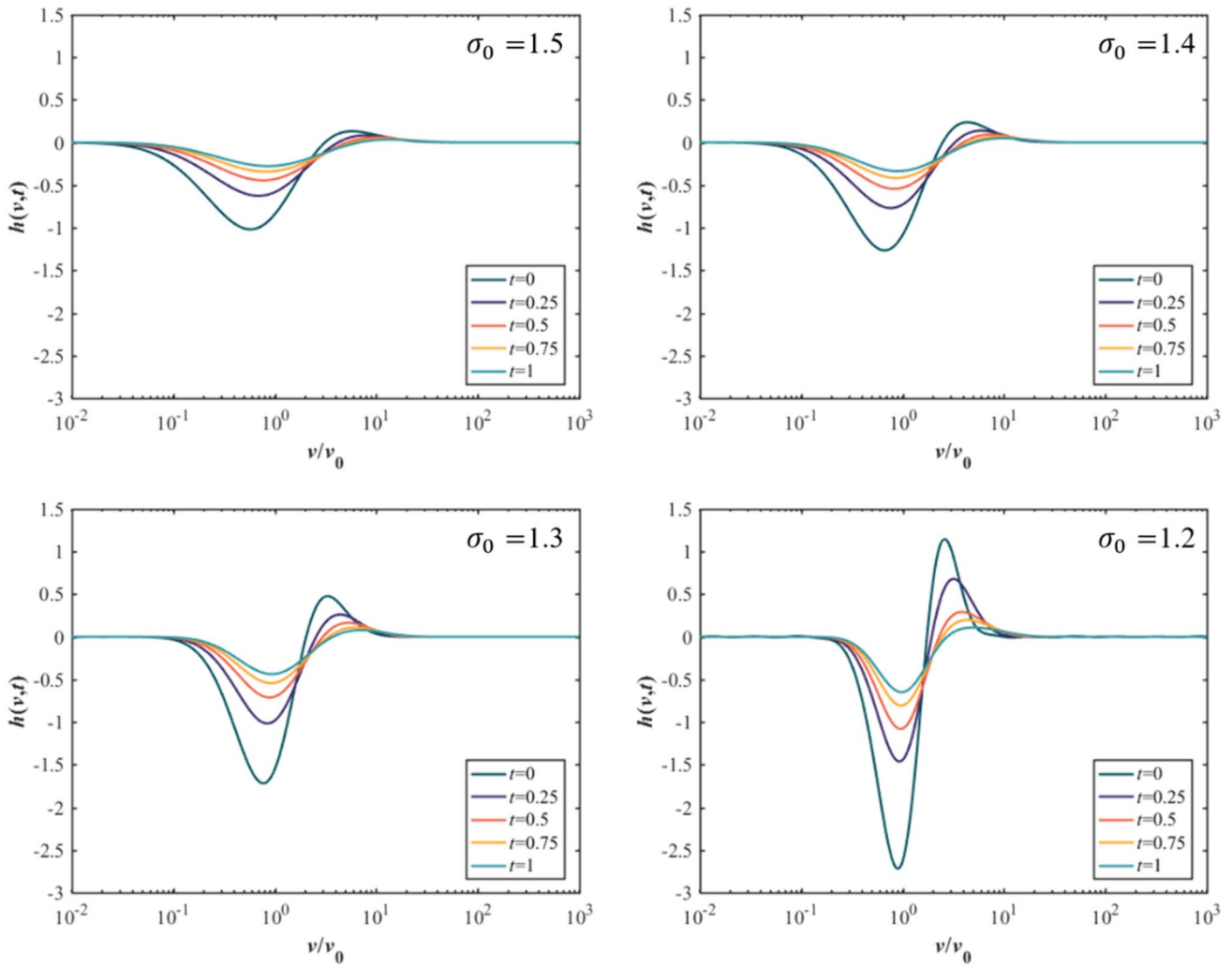
Fig. 6 The $h(v, t)$ of different initial GSD calculated by the RBF method in the continuum regime
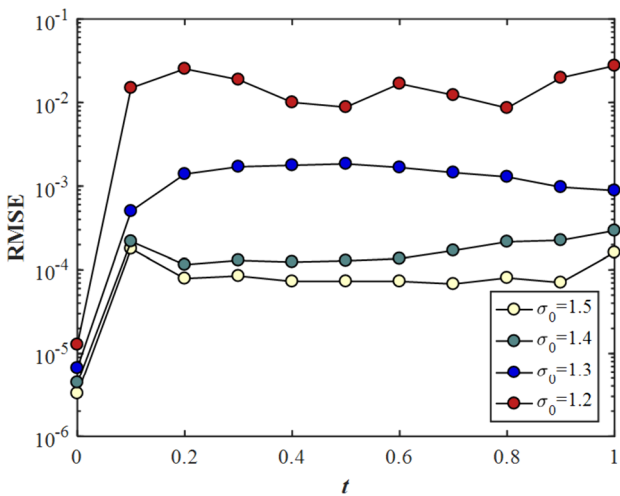

Fig. 7 In the continuum regime, the RMSE is calculated for different initial GSD using the RBF method
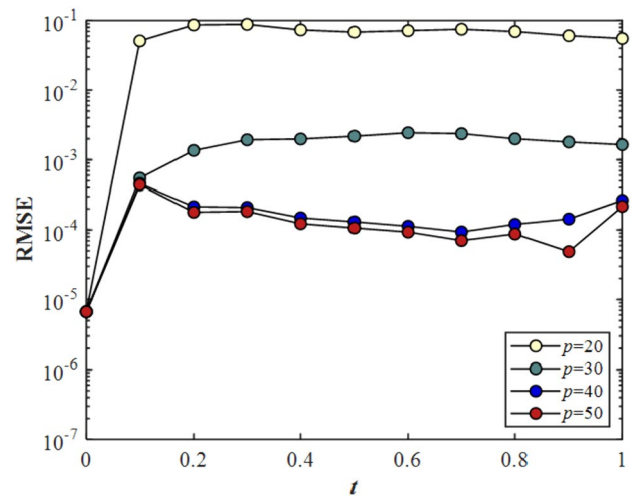
Fig. 8 The error corresponding to the calculation results of different numbers of basis functions

of solving the PBE using RBF, the standard deviation of the basis functions was often determined according to Eqs. (9) and (10). This configuration method generally yields satisfactory results in most cases. However, in practice, for calculating cases with lower GSD, the strategy of adjusting the shape of basis functions often proves effective in improving result accuracy. To investigate the effect of standard deviation on the initial GSD at low values, different standard deviations were used for calculations. The parameter settings remained consistent with those in Sect. 4.1. The $h(v, t)$ is as follows:

It can be seen from Fig. 9 that when $\sigma_v = 0.198$, the computed results are not smooth due to the small standard deviation of the basis functions. For a too-small standard deviation, the model excessively adapts to the training samples but fails to capture the overall pattern of the data. This manifests as the model meeting the PBE constraints only at the training sample points, while struggling to generalize well elsewhere. When $\sigma_v = 0.992$, the basis

function becomes flat. This makes it difficult for the basis function to accurately capture gradient changes (Fornberg and Zuev 2007).

Figure 10 shows the RMSE corresponding to various σ_v:

Figure 10 shows that the influence of the shape of the basis function on the efficiency of RBF calculation is obvious. To improve the accuracy of estimation for steep functions, a smaller standard deviation can be selected. Smaller standard deviation allows the basis function to better capture gradients and reduce calculation errors. However, if the standard deviation is too small, it will reduce the complexity of the model, make the generalization performance of the trained model worse, and overfitting is more likely to occur. Simultaneously, if the basis functions are too narrow, it may be necessary to employ a greater number of them to cover the data adequately, which can increase the computational costs of the model (Fasshauer 2007). In cases where the initial
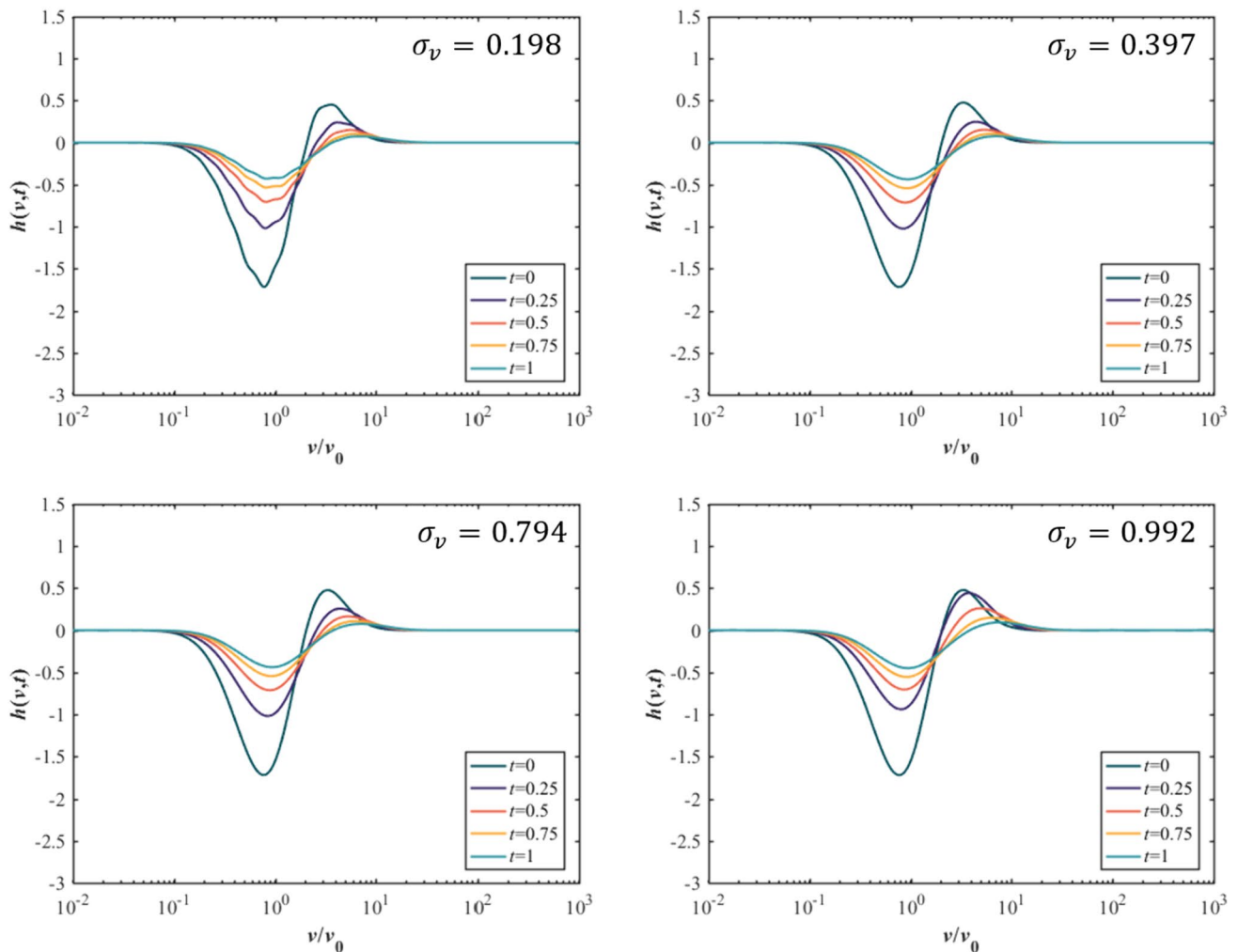

Fig. 9 The $h(v, t)$ corresponding to the calculation results of basis functions with different standard deviation
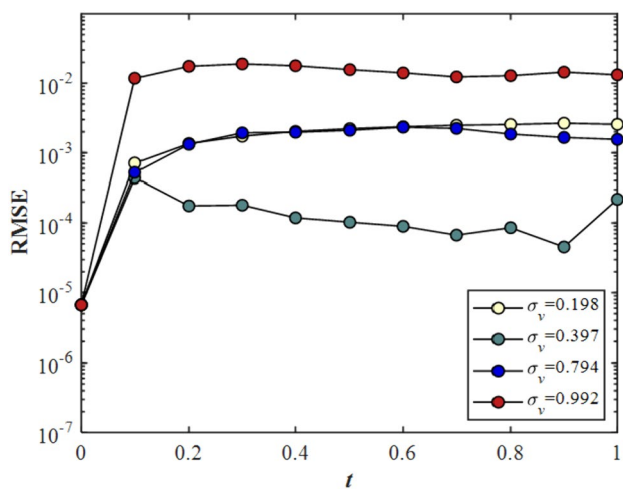
Fig. 10 The error corresponding to the calculation results of basis functions with different shape

GSD is small, the standard deviation can be appropriately reduced to ensure the accuracy of the calculation.

4.4 Effect of Fractal Dimension on Error Generation

We observed that the choice of D_f values influences the computational outcomes of the RBF method. Consequently, we computed results for different D_f values to facilitate comparison. Given that the impact of D_f varies in the continuum regime and free molecular regime on the particle number density function, separate computations were conducted in these regions. The computational parameters remained consistent with those outlined in Sects. 4.1 and 4.2. The range for D_f was selected from 1.5 to 3.

Figure 11 shows the $h(v,t)$ of the different D_f constructed by the RBF method.
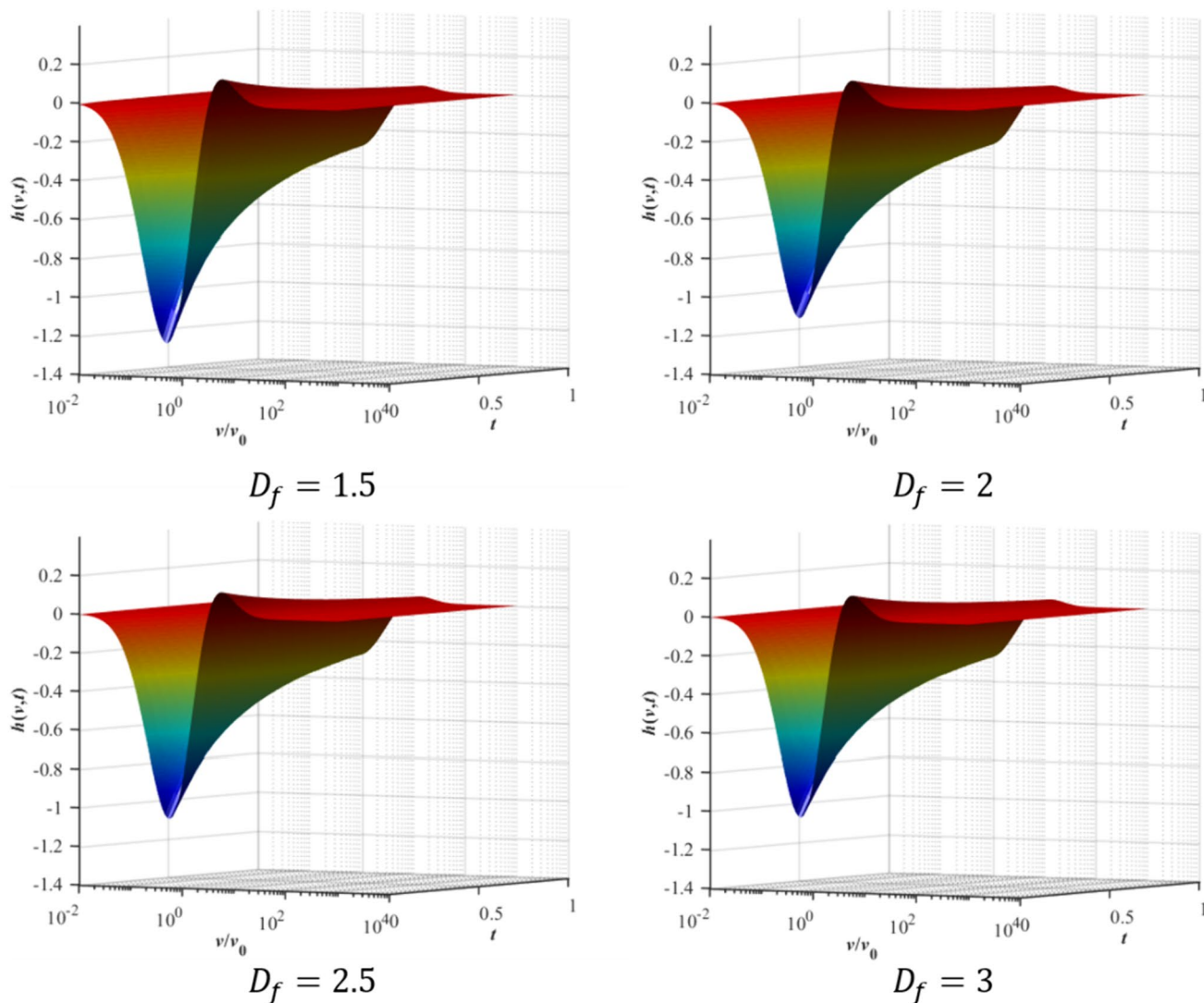

Fig. 11 The calculated $h(v,t)$ of different D_f by the RBF method in the continuum regime

Based on the computational results in Sect. 4.1, the influence of D_f in the continuum regime on the particle number density function is relatively small. Therefore, as depicted in Fig. 11, reducing D_f shapes $h(v,t)$ to become steeper, but the magnitude of the change is not significant.

Figure 12 shows the RMSE of the D_f corresponding to Fig. 11.

In Sect. 4.3, we observed that an increase in local gradients leads to a decrease in the accuracy of the RBF method. The choice of D_f values affects the accuracy of RBF due to this reason as well. The variation of D_f causes changes in the local gradient of $h(v,t)$ in the temporal direction, thereby leading to the generation of errors. Figure 12 illustrates that RMSE increases with the decrease of D_f, which means that the effect of the RBF method calculation becomes worse. However, since the D_f has a relatively small impact on PSD in the continuum regime, the RMSE does not change significantly.

Figure 13 shows the $h(v,t)$ of the different D_f constructed by the RBF method in the free molecular regime.

From Fig. 13, it can be observed that in the free molecular regime, as the value of D_f decreases, the function plot of $h(v,t)$ becomes steeper. Since the evolution of agglomerate particle size in the free molecular regime is significantly influenced by the D_f, the changes in the $h(v,t)$ plot are more pronounced compared to the continuum regime.

Figure 14 shows the RMSE of different D_f corresponding to Fig. 13. The RMSE curve at $D_f = 1.5$ is not listed here because the SM is difficult to calculate when the initial GSD = 1.5 and $D_f = 1.5$.

Figure 14 also shows a similar trend to Fig. 12, as the D_f becomes smaller, the calculation error of the RBF method is increasing. This implies that the variations in $h(v,t)$
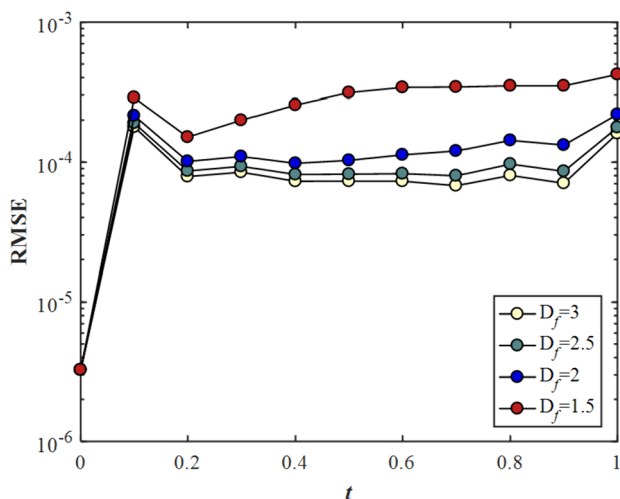
lead to a decrease in accuracy for the RBF method in the free molecular regime as well. Simultaneously, due to the significant impact of D_f on the particle number density function in the free molecular regime, the computational accuracy in this region is comparatively lower than in the continuum regime. Therefore, the RBF method is more suitable for the case of large D_f. Furthermore, special attention should be given to adjusting the parameters of the basis functions based on the variations in D_f when computing in the free molecular regime, ensuring the accuracy of the calculation results.

4.5 Efficiency

Tables 1 and 2 respectively present the computation time and accuracy of the RBF method, corresponding to the computational scenarios outlined in Sects. 4.1 and 4.2. In the iterative process of using the LM algorithm, when the value of the Eq. (18) is less than 1e−9 or the LM algorithm iterates 100 times, the iteration is stopped early.

By comparing the calculation efficiency in the table, it is found that although the calculation accuracy is slightly decreased in the process of D_f from 3 to 2, the accuracy and speed can still meet the basic requirements, which is still a great advantage compared with SM in speed.

5 Conclusions

The RBF method is initially employed to examine the dynamics of fractal-like agglomerates. This study explores the method's applicable conditions, advantages, and disadvantages. Firstly, it investigates two dynamical processes of fractal-like agglomerates. Secondly, it explores the impacts of various initial GSD and D_f values on the computational efficiency and accuracy of the RBF method. From the calculation results of the RBF method for different D_f in continuum regime and free molecular regime, this method can directly calculate the size distribution of agglomerates in a limited area and maintain high accuracy and speed.

By comparing different initial GSD calculation examples, the RBF method is more suitable for calculating the initial GSD with a large value. When the initial GSD continues to become smaller, the RBF method needs to increase the number of basis functions or adjust the basis function standard deviation to ensure the accuracy of the calculation.

By comparing the calculation examples of different D_f in the free molecular regime and continuum regime, it is found that the RBF method is more suitable for the case where the D_f is larger. Whether it is in the continuum regime or the free molecular regime, the efficacy of the RBF method diminishes as the value of D_f decreases, and the calculation
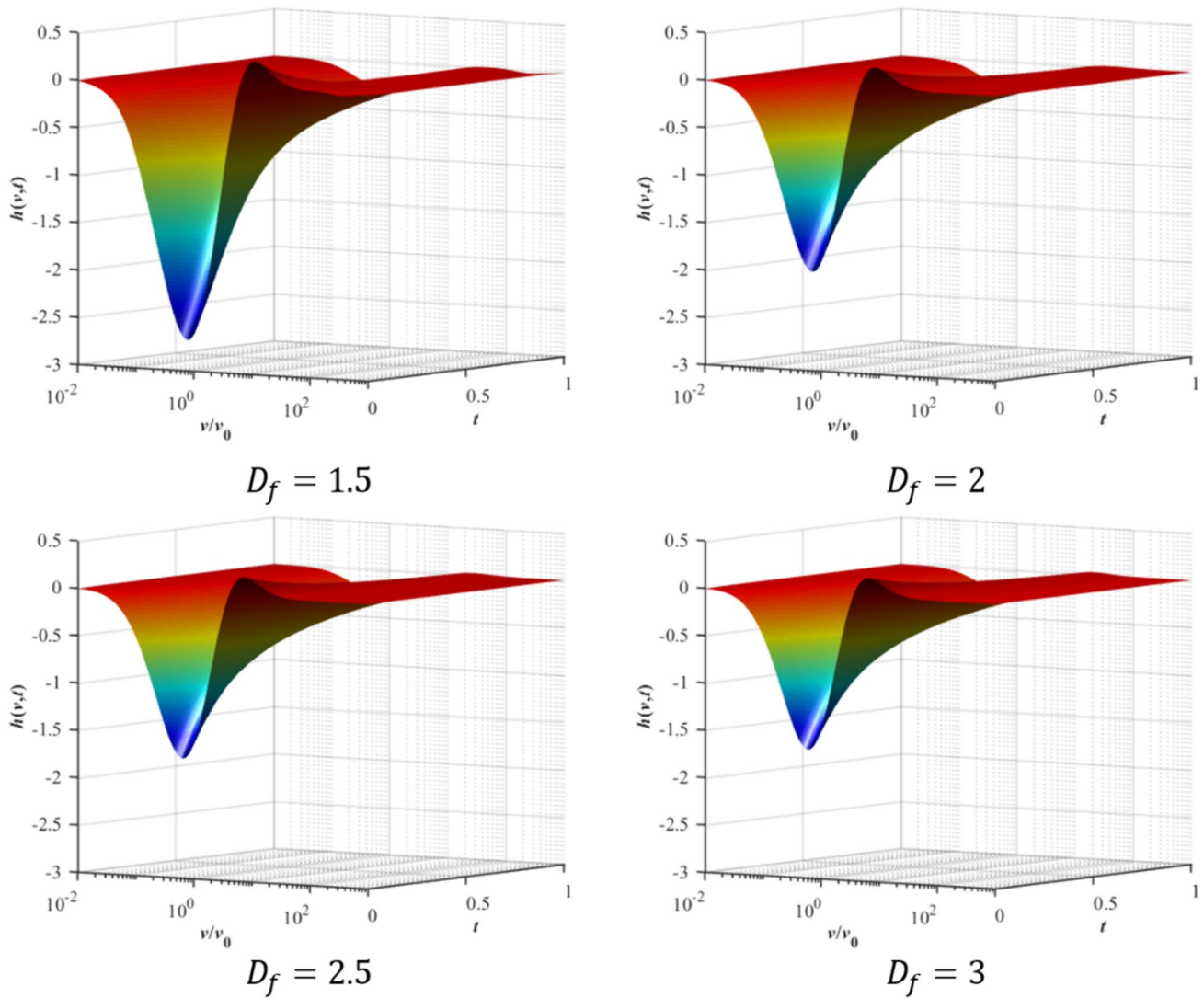

Fig. 12 In continuum regime, the RMSE is calculated using the RBF method of different D_f

Fig. 13 The calculated $h(v, t)$ of different D_f by the RBF method in the free molecular regime
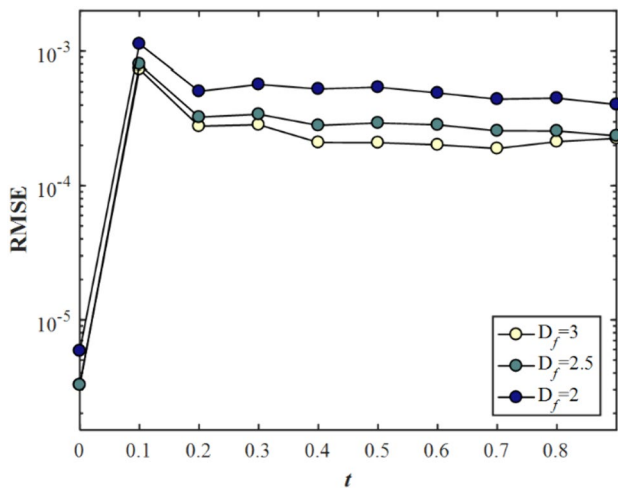

Fig. 14 In the free molecular regime, the RMSE of different D_f is calculated using the RBF method

Table 1 Comparison of the continuum regime calculation efficiency

D_f	RMSE	RBF computational time	SM computational time
3.0	9.7982e−05	5.979 s	10 h
2.5	1.0223e−04	5.940 s	10 h
2.0	1.6393e−04	5.355 s	10 h

effect in the free molecular regime is more affected by D_f than in the continuum regime.

Table 2 Comparison of the free molecular regime calculation efficiency

D_f	RMSE	RBF computational time	SM computational time
3.0	2.4593e−04	5.728 s	10 h
2.5	3.1836e−04	6.543 s	10 h
2.0	5.2012e−04	8.234 s	10 h

Declarations

Conflict of Interest The authors declare that they have no known competing financial interests or personal relationships that could have appeared to influence the work reported in this paper.

References

Alzyod S (2021) The adaptive radial basis method (ARBM): an application to the hydrodynamics of liquid-liquid dispersions. Elsevier Masson SAS. https://doi.org/10.1016/B978-0-323-88506-5.50078-4

Alzyod S, Charton S (2020) A meshless Radial Basis Method (RBM) for solving the detailed population balance equation. Chem Eng Sci 228:115973. https://doi.org/10.1016/j.ces.2020.115973

Apelgren P, Amoroso M, Säljö K, et al. (2019) Investigations on electrochemical machining (ECM) of Al7075 material using copper electrode for improving geometrical tolerance. Mater Today Proc 27(xxxx): 0–31. https://doi.org/10.1016/j.matpr.2019.12.188

Bayona V, Moscoso M, Kindelan M (2011) Optimal constant shape parameter for multiquadric based RBF-FD method. J Comput Phys 230(19):7384–7399

Fasshauer GE (2007) Meshfree approximation methods with MATLAB. World Scientific

Fornberg B, Zuev J (2007) The Runge phenomenon and spatially variable shape parameters in RBF interpolation. Comput Math with Appl 54(3):379–398

Fox RO, Laurent F, Passalacqua A, et al. (2022) The generalized quadrature method of moments to cite this version : HAL Id : hal-03762976. The Generalized Quadrature Method of Moments. Epub ahead of print 2022.

Friedlander SK (2000) Smoke, dust and haze: fundamentals of aerosol dynamics, 2nd edn. Oxford University Press, Oxford

Harris M, Kassab A, Divo E (2017) An RBF interpolation blending scheme for effective shock-capturing. Int J Comput Methods Exp Meas 5(3):281–292

Hinds WC, Zhu Y (2022) Aerosol technology: properties, behavior, and measurement of airborne particles. Wiley

Jeldres RI, Fawell PD, Florio BJ (2018) Population balance modelling to describe the particle aggregation process: a review. Powder Technol 326:190–207. https://doi.org/10.1016/j.powtec.2017.12.033

Kuo L-H (2015) On the Selection of a Good Shape Parameter for RBF Approximation and Its Application for Solving PDEs. The University of Southern Mississippi

Mirzaei D (2020) The direct radial basis function partition of unity (d-rbf-pu) method for solving pdes. 2019(98012657): 1–30

Motaman F, Rakhshandehroo GR, Hashemi MR et al (2018) Application of RBF-DQ method to time-dependent analysis of unsaturated seepage. Transp Porous Media 125(3):543–564. https://doi.org/10.1007/s11242-018-1138-7

Mountain RD, Mulholland GW, Baum H (1986) Simulation of aerosol agglomeration in the free molecular and continuum flow regimes. J Colloid Interface Sci 114(1):67–81

Müller H (1928) Zur allgemeinen theorie ser raschen koagulation. Kolloidchem Beihefte 27(6–12):223–250

Rodrigues P, Franzelli B, Vicquelin R et al (2018) Coupling an LES approach and a soot sectional model for the study of sooting turbulent non-premixed flames. Combust Flame 190:477–499. https://doi.org/10.1016/j.combustflame.2017.12.009

Sarra SA, Bai Y (2018) A rational radial basis function method for accurately resolving discontinuities and steep gradients. Appl Numer Math 130:131–142. https://doi.org/10.1016/j.apnum.2018.04.001

Sarra SA, Sturgill D (2009) A random variable shape parameter strategy for radial basis function approximation methods. Eng Anal Bound Elem 33(11):1239–1245

Smoluchowski MV (1918) Versuch einer mathematischen theorie der Koagulationskinetik kolloider Lösungen. Zeitschrift Für Phys Chemie 92U(1):129–168

Uddin M (2014) On the selection of a good value of shape parameter in solving time-dependent partial differential equations using RBF approximation method. Appl Math Model 38(1):135–144. https://doi.org/10.1016/j.apm.2013.05.060

Vemury S, Pratsinis SE (1995) Self-preserving size distributions of agglomerates. J Aerosol Sci 26(2):175–185

Wang K, Yu S, Peng W (2020) A new method for solving population balance equations using a radial basis function network. Aerosol Sci Technol 54(6):644–655. https://doi.org/10.1080/02786826.2019.1711358

Wang K, Hu R, Xiong Y et al (2022) Radial basis function method for predicting the evolution of aerosol size distributions for coagulation problems. Atmos (Basel) 13(11):1895

Xie M-L, Yu M-Z, Wang L-P (2012) A TEMOM model to simulate nanoparticle growth in the temporal mixing layer due to Brownian coagulation. J Aerosol Sci 54:32–48

Yu M, Lin J (2009a) Solution of the agglomerate Brownian coagulation using Taylor-expansion moment method. J Colloid Interface Sci 336(1):142–9

Yu M, Lin J (2009b) Taylor-expansion moment method for agglomerate coagulation due to Brownian motion in the entire size regime. J Aerosol Sci 40(6):549–562

Yu M, Lin J, Chan T (2008) A new moment method for solving the coagulation equation for particles in Brownian motion. Aerosol Sci Technol 42(9):705–713

Yu M, Liu Y, Jin G et al (2016) A new analytical solution for agglomerate growth undergoing Brownian coagulation. Appl Math Model 40:5497–5509

Yu M, Lin J, Seipenbusch M et al (2017) Verification of size-resolved population balance modeling for engineered nanoparticles under high concentration. Chem Eng J 323:592–604. https://doi.org/10.1016/j.cej.2017.04.128